Random replicators with asymmetric couplings

2006 J. Phys. A: Math. Gen. 39 3853

(http://iopscience.iop.org/0305-4470/39/15/001)

INSTITUTE OF PHYSICS PUBLISHING JOURNAL OF PHYSICS A: MATHEMATICAL AND GENERAL

J. Phys. A: Math. Gen. **39** (2006) 3853–3869 doi:10.1088/0305-4470/39/15/001

Random replicators with asymmetric couplings

Tobias Galla

The Abdus Salam International Centre for Theoretical Physics, Strada Costiera 11, 34014 Trieste, Italy
and
CNR-INFM, Trieste-SISSA Unit, V. Beirut 2-4, 34014 Trieste, Italy

E-mail: galla@ictp.trieste.it

Received 15 August 2005, in final form 30 January 2006
Published 29 March 2006
Online at stacks.iop.org/JPhysA/39/3853

Abstract

Systems of interacting random replicators are studied using generating functional techniques. While replica analyses of such models are limited to systems with symmetric couplings, dynamical approaches as presented here allow us specifically to address cases with asymmetric interactions where there is no Lyapunov function governing the dynamics. We focus on replicator models with Gaussian couplings of general symmetry between $p \geqslant 2$ species, and discuss how an effective description of the dynamics can be derived in terms of a single-species process. Upon making a fixed point ansatz persistent order parameters in the ergodic stationary states can be extracted from this process, and different types of phase transitions can be identified and related to each other. We discuss the effects of asymmetry in the couplings on the order parameters and the phase behaviour for $p = 2$ and $p = 3$. Numerical simulations verify our theory. For the case of cubic interactions, numerical experiments indicate regimes in which only a finite number of species survives, even when the thermodynamic limit is considered.

PACS numbers: 87.23.−n, 87.10.+e, 75.10.Nr, 64.60.Ht

1. Introduction

Replicator equations describe the evolution of self-reproducing interacting species within a given framework of limited resources. They have found wide applications in a variety of fields including evolutionary game theory, socio-biology, pre-biotic evolution, optimization theory and population dynamics, where equivalences to Lotka–Volterra equations can be established [1–3]. So-called random replicator models (RRMs) are also interesting from the point of view of statistical mechanics, as they constitute complex disordered systems with non-trivial co-operative behaviour such as phase transitions, ergodicity breaking and memory effects.

Statistical physics can contribute to the analysis of large systems of replicators with quenched interactions. Stochastic couplings drawn at random from some fixed probability distribution here reflect a lack of knowledge of the detailed interactions of real replicator systems. The tools also used for the analysis of disordered systems in the physics context, are then well suited to compute typical properties of such random replicator models, i.e. averages of observables over the distribution of couplings.

The first replicator system with quenched random couplings was introduced and studied with path integral methods by Diederich and Opper in [4–6]. Most subsequent studies in the statistical physics community were then based either on replica theory or purely on computer simulations [7–15].

The restriction to replica methods severely limits the types of models that can be addressed, as static analyses require the existence of a global Lypunov (or energy) function which is extremized by the replicator dynamics. This in turn requires the interaction matrix of the replicators (for pairwise interaction denoted by J_{ij}) to be symmetric against permutations of the interacting species, $J_{ij} = J_{ji}$ (generalization to higher order interactions is straightforward and will be discussed below). This appears unrealistic in both the game-theoretic and the biological contexts.

In the framework of evolutionary game theory, replicator equations describe the evolution of one or several populations of players, who engage in a game which is played repeatedly [3]. The interaction matrices here encode the payoffs given to the individual players, and these then reproduce according to their success. In the simplest case of two players i and j participating in the game, J_{ij} would denote the payoff of player i when playing against j, and J_{ji} the corresponding payoff for j. Replica theory can here be applied to the resulting replicator model only when $J_{ij} = J_{ji}$ for all pairs (i, j) of players. This corresponds to equal payoffs for both players, which does not appear to be the typical situation in real games. On the contrary one would like to introduce an anti-correlation between J_{ij} and J_{ji} so that player i's payoff is positive, whenever j's is negative and vice versa. In particular, zero-sum games correspond to the case $J_{ij} = -J_{ji}$ i.e., full anti-correlation. Similarly, the $\{J_{ij}\}$ in biological applications describe interactions between different species. The fully symmetric case here corresponds to either reciprocal stimulation or reciprocal inhibition, which again is unrealistic, as prey–predator relations between two species i and j would, for example, require J_{ij} and J_{ji} to be of opposite signs.

To address replicator systems with fully or partially asymmetric couplings, methods other than replica theory are required. The only existing analytical studies here appear to be the early papers by Rieger [16] and by Opper and Diederich [5, 6], where RRMs were studied using generating functional techniques.

Such dynamical methods are not concerned with the extremization of a Lyapunov function, but address the temporal evolution of the system directly. Generating functionals therefore provide a powerful tool to deal with non-equilibrium disordered systems lacking detailed balance. While they were originally developed to study magnetic phenomena in spinglasses [17, 18], they have recently also been applied to models of interacting agents, for example, in the so-called Minority Game [19–21].

The aim of this paper is to discuss dynamical methods in the context of random replicator models and to extend the work of [5, 6] (which is concerned with pairwise Gaussian interactions) to more general Gaussian replicator systems. To this end, we work out the effective description of the dynamics of such RRMs in terms of a single-species process, and then extract the relevant order parameters in the resulting fixed point states, on the basis of an ergodicity assumption. The breakdown of ergodicity in turn signals the onset of memory effects, and we compute the corresponding phase diagrams. Some differences in the types of

transitions are here observed depending on the symmetry of the couplings and the order of the interactions (e.g., pairwise versus higher order). Our study is in direct extension also of [7], where the case of higher order symmetric couplings with Gaussian distribution was addressed using replica theory.

2. Model definitions

We consider replicator systems of N interacting species labelled by Roman indices $i = 1, \ldots, N$ with time-dependent concentrations $x_i(t) \geqslant 0$. Replicator equations are generally of the form

$$\frac{\mathrm{d}}{\mathrm{d}t}x_i(t) = x_i(t)(f_i[\mathbf{x}(t)] - f[\mathbf{x}(t)]) \tag{1}$$

with $f_i[\mathbf{x}]$ the 'fitness' or 'success' of species i (which may depend on the concentrations $\mathbf{x} = (x_1, \ldots, x_N)$ of all species). $f[\mathbf{x}]$ in turn denotes the 'mean' fitness $f[\mathbf{x}] = \sum_i x_i f_i[\mathbf{x}]$. Thus, the concentration of species who are fitter than the average increases, and the weight of species less fit than average decreases. Note that equation (1) conserves the total concentration $\sum_i x_i(t) = 1$.

We will here focus on systems with second and higher order interactions, with couplings drawn from a Gaussian distribution, i.e. we will consider replicator equations of the form

$$\frac{\mathrm{d}}{\mathrm{d}t}x_i(t) = -x_i(t)\left[2ux_i(t) + \sum_{(i_2,\ldots,i_p)\in M_i^{(p)}} J^i_{i_2,i_3,\ldots,i_p}x_{i_2}(t)x_{i_3}(t)\cdots x_{i_p}(t) - \kappa(t) - h(t)\right] \tag{2}$$

with p a fixed integer and where $M_i^{(p)} = \{(i_2, \ldots, i_p){:}1 \leqslant i_2 < i_3 < \cdots < i_p \leqslant N;\ i_2, \ldots, i_p \neq i\}$. Note the overall negative sign introduced for later convenience.

The first (diagonal) term in the square brackets describes a self-interaction. Such terms were first introduced in the context of replicator models in [2]. Depending on the value of the model parameter $u \geqslant 0$, the so-called co-operation pressure, the growth of any single individual concentration is either strongly or only moderately suppressed (large versus small values of u respectively). Given the fixed total concentration of species large values of u hence drive the system towards a co-operative state in which many species survive at small individual concentrations, whereas small co-operation pressure can lead to stationary states in which a large fraction of the species dies out asymptotically and where the remaining ones operate at high concentrations. In terms of game theory, this corresponds to states in which many or few pure strategies are being played respectively [3]. In the limit $u \to \infty$ the only stable attractor is given by a fixed point at which all species carry equal weight.

The second term in the square bracket of (2) describes the interaction between species. The couplings $\{J\}$ are assumed to be drawn from a Gaussian distribution with zero mean and with variance and correlations as follows [23]:

$$\overline{\left(J^{i_1}_{i_2,\ldots,i_p}\right)^2} = \frac{p!}{2N^{p-1}}, \qquad \overline{J^{i_1}_{i_2,\ldots,i_p}J^{i_k}_{i_1,\ldots,i_{k-1},i_{k+1},\ldots,i_p}} = \Gamma\frac{p!}{2N^{p-1}}. \tag{3}$$

$\overline{\cdots}$ denotes an average over the distribution of the couplings. $\Gamma \in [-1, 1]$ is a symmetry parameter. For $\Gamma = 1$ their distribution is fully symmetric with respect to permutations of the indices, $\Gamma = 0$ corresponds to the case of fully uncorrelated couplings and $\Gamma = -1$ to the fully anti-correlated case. Choosing $-1 \leqslant \Gamma \leqslant 1$ allows one to interpolate smoothly between the different regimes. In the case of pairwise interactions $p = 2$ the choice $\Gamma = -1$ corresponds to $J_{ij} = -J_{ji}$, i.e. to zero-sum games as mentioned in the introduction. For $p > 2$ the value

$\Gamma = -1$ cannot be realized, since, e.g. for $p = 3$ it is impossible to draw three couplings all being equal in their absolute values but with pairwise opposite signs.

The field $h(t)$ in equation (2) has been introduced to generate response functions in the course of the dynamical analysis of the system. It will be set to zero at the end of the calculation.

Finally, up to a sign the normalization parameter $\kappa(t)$ corresponds to the mean fitness $f[\mathbf{x}]$ mentioned above and is chosen to ensure the constraint

$$\frac{1}{N}\sum_i x_i(t) = 1 \tag{4}$$

at any time t. We choose initial conditions such that this constraint is fulfilled at the starting point $t = 0$. Note that we have here re-scaled the concentrations such that $\sum_i x_i = N$ instead of $\sum_i x_i = 1$; this is to ensure appropriate scaling of the statistical mechanics quantities and a well-defined thermodynamic limit.

3. Generating functional analysis and fixed-point solutions

3.1. Effective theory

Equations (2) define a set of N evolution equations, which are coupled to each other through the random interactions $\mathbf{J}$, and through the overall constraint (4). A Lyapunov function governing this dynamics can be found only in the case of symmetric couplings $\Gamma = 1$. In the following we will apply generating functionals originally developed by De Dominicis [17] to obtain a macroscopic description of the coupled N-species dynamics.

To this end one defines a dynamical generating functional

$$\begin{aligned} Z[\psi] &= \left\langle\!\left\langle \exp\left(\mathrm{i}\sum_i \int \mathrm{d}t\, \psi_i(t)x_i(t)\right)\right\rangle\!\right\rangle \\ &= \int D\mathbf{x} p_0(\mathbf{x}(0)) \exp\left(\mathrm{i}\sum_i \int \mathrm{d}t\, \psi_i(t)x_i(t)\right)\prod_{i,t}\delta[\text{Equation (2)}]. \end{aligned} \tag{5}$$

$\langle\langle\cdots\rangle\rangle$ denotes an average over all possible paths of the system. $p_0(\mathbf{x}(0))$ describes the (possibly random) initial conditions from which the dynamics is started. All initial concentrations are taken to be strictly positive with probability 1 here, and we assume in the following that the distribution of initial conditions factorizes over individual species, i.e. $p_0(\mathbf{x}(0)) = \prod_i p_0(x_i(0))$.

The general procedure then consists in a computation of the disorder-averaged generating functional $\overline{Z[\psi]}$, from which dynamical order parameters can be computed as derivatives with respect to the fields $\{\psi_i(t), h(t)\}$. The aim is to formulate a closed set of equations describing the temporal evolution of a suitable set of dynamical observables, which adequately describe the macroscopic dynamics. The relevant order parameters for the RRMs considered here are given by the Lagrange parameter $\boldsymbol{\kappa} = \{\overline{\langle\kappa(t)\rangle}\}$ and the correlation and response functions $\{\mathbf{C}, \mathbf{G}\}$ in the thermodynamic limit:

$$C(t,t') = \lim_{N\to\infty}\frac{1}{N}\sum_{i=1}^N \overline{\langle x_i(t)x_i(t')\rangle}, \qquad G(t,t') = \lim_{N\to\infty}\frac{1}{N}\sum_{i=1}^N \overline{\left\langle\frac{\delta x_i(t)}{\delta h(t')}\right\rangle}. \tag{6}$$

Here $\langle\cdots\rangle$ stands for an average over realizations of the possibly randomly drawn initial conditions. Note that $G(t,t') = 0$ for $t \leqslant t'$ because of causality.

The evaluation of the disorder average in the generating functional can be carried out along the lines of [24] after a transformation $y_i(t) = \log x_i(t)$ has been performed. The calculation is straightforward, but lengthy. We will therefore not enter into the details of the mathematical derivation here, but will only report the final outcome.

One finds that a description of the dynamics can be obtained in terms of an effective process of the form

$$\frac{\mathrm{d}}{\mathrm{d}t}x(t) = -x(t)\left[2ux(t) - \Gamma\frac{p(p-1)}{2}\int_0^t \mathrm{d}t' G(t,t')C(t,t')^{p-2}x(t') + \eta(t) - \kappa(t) - h(t)\right]. \tag{7}$$

This equation describes a stochastic process for a representative species concentration $\{x(t)\}$, which is a random variable and subject to Gaussian noise $\{\eta(t)\}$, with non-trivial temporal correlations according to the following equation:

$$\langle \eta(t)\eta(t')\rangle_\star = \frac{p}{2}C(t,t')^{p-1}. \tag{8}$$

The correlation and response functions $\mathbf{C}$ and $\mathbf{G}$ of the original multi-species system (see equation (6)) can in turn be shown to be given by

$$C(t,t') = \langle x(t)x(t')\rangle_\star, \qquad G(t,t') = \left\langle \frac{\delta x(t)}{\delta h(t')}\right\rangle_\star, \tag{9}$$

and $\boldsymbol{\kappa}$ in (7) has to be chosen such that

$$\langle x(t)\rangle_\star = 1 \qquad \forall t. \tag{10}$$

$\langle\cdots\rangle_\star$ denotes an average over realizations of the effective process (7), i.e., over realizations of the single-species coloured noise $\{\eta(t)\}$ and over initial conditions described by $p_0(x(0))$.

Equations (7)–(10) thus form an implicit, but closed, set of equations from which $\{\boldsymbol{\kappa}, \mathbf{C}, \mathbf{G}\}$ are to be obtained. For $p = 2$ this system coincides with the results of [5]. The description in terms of an ensemble of decoupled, but stochastic effective species is exact and fully equivalent to the original N-species problem (defined by equation (2)) in the limit $N \to \infty$ (in the sense that disorder averages of macroscopic observables in the original dynamics can be obtained as averages $\langle\cdots\rangle_\star$ on the level of the effective process). The retarded self-interaction and the coloured noise in the effective process are direct consequences of the quenched disorder in the original problem and impede a full explicit analytical solution of the self-consistent saddle-point problem for the two-time quantities $C(t,t')$ and $G(t,t')$ and the full function $\kappa(t)$. One is therefore limited to a specific ansatz for the trajectories of the effective particles.

3.2. Fixed-point solutions

To proceed analytically we assume that the system reaches a fixed point asymptotically, i.e. $x_i(t) \to x_i$ as $t \to \infty$ for all i in the original dynamics. Numerical simulations confirm that this assumption is indeed justified for values of u larger than some critical value u_c (the value of u_c may depend on p and Γ as discussed in detail below).

We may then make a similar assumption for the realizations of the effective process, i.e. $x(t) \to x$, with x a static random variable. Accordingly, the correlation function becomes flat at the fixed point and $\kappa(t)$ approaches a fixed point as well, so that we write

$$\lim_{t\to\infty} C(t+\tau,t) = q \quad \forall\tau, \qquad \lim_{t\to\infty}\kappa(t) = \kappa. \tag{11}$$

We also make the standard ansatz of a time-translation invariant asymptotic response function

$$\lim_{t\to\infty} G(t+\tau,t) = G(\tau). \tag{12}$$

Furthermore, we will address only ergodic stationary states, i.e. states in which perturbations have no long-term effects so that the integrated response function remains finite

$$\chi \equiv \int_0^\infty \mathrm{d}\tau\, G(\tau) < \infty, \tag{13}$$

and no long-term memory is present, i.e., we will assume

$$\lim_{t\to\infty} G(t,t') = 0 \tag{14}$$

also for finite t'. In the absence of memory we may send the starting point of the dynamics to $-\infty$ for convenience.

Finally, within the fixed-point ansatz we also assume that each realization of the the single-species noise $\{\eta(t)\}$ approaches a time-independent value η asymptotically, which according to (8) is then a static Gaussian variable with zero mean and variance

$$\langle \eta^2 \rangle_\star = \frac{p}{2} q^{p-1}. \tag{15}$$

Fixed points of (7) then fulfil the condition

$$x\left(2ux - \Gamma\frac{p(p-1)}{2}q^{p-2}\chi x + \left(\frac{p}{2}q^{p-1}\right)^{1/2} z - \kappa\right) = 0, \tag{16}$$

where we have written $\eta = \left(\frac{p}{2}q^{p-1}\right)^{1/2} z$ with z a standard Gaussian variable. $h(t)$ has been set to zero at this stage (derivatives with respect to $h(t)$ can be obtained as derivatives with respect to the effective-particle noise $\eta(t)$ up to an inverted sign). We note that $x(z) = 0$ is a solution of this equation for all the realizations of the random variable z. Other solutions may be possible whenever setting the bracket to zero leads to a positive value of $x(z)$. Taking into account the stability of the zero solutions, one finds that the ansatz

$$x(z) = \frac{\kappa - \left(\frac{p}{2}q^{p-1}\right)^{1/2} z}{2u - \Gamma p(p-1)\chi q^{p-2}/2}\Theta\left[\kappa - \left(\frac{p}{2}q^{p-1}\right)^{1/2} z\right] \tag{17}$$

adequately describes the solutions, with $\Theta[x]$ the step function ($\Theta[x] = 1$ for $x > 0$ and $\Theta[x] = 0$ otherwise). In a manner similar to [5, 28] one demonstrates that zero fixed points $x(z) = 0$ are unstable for positive arguments of the Θ-function. Self-consistency then demands that

$$\int \mathrm{D}z\, x(z) = 1, \qquad \int \mathrm{D}z\, x(z)^2 = q, \qquad -\left(\frac{p}{2}q^{p-1}\right)^{-1/2} \int \mathrm{D}z \frac{\partial x(z)}{\partial z} = \chi \tag{18}$$

with $\mathrm{D}z = \frac{\mathrm{d}z}{\sqrt{2\pi}} e^{-z^2/2}$ a standard Gaussian measure. Upon using the explicit ansatz (17) for the fixed points these equations may be written as

$$\left(\frac{p}{2}q^{p-1}\right)^{-1/2}\left(2u - \Gamma\frac{p(p-1)}{2}\chi q^{p-2}\right) = \int_{-\infty}^{\Delta} \mathrm{D}z(\Delta - z), \tag{19}$$

$$q\left(\frac{p}{2}q^{p-1}\right)^{-1}\left(2u - \Gamma\frac{p(p-1)}{2}\chi q^{p-2}\right)^2 = \int_{-\infty}^{\Delta} \mathrm{D}z(\Delta - z)^2, \tag{20}$$

$$\left(2u - \Gamma\frac{p(p-1)}{2}\chi q^{p-2}\right)\chi = \int_{-\infty}^{\Delta} \mathrm{D}z, \tag{21}$$

with $\Delta = \kappa/\left(\frac{p}{2}q^{p-1}\right)^{1/2}$. We note that $\phi = \int_{-\infty}^{\Delta} \mathrm{D}z$ represents the probability of a given species i to survive in the long-term limit, i.e., to attain a fixed point value $x_i = \lim_{t\to\infty} x_i(t) > 0$. We will refer to ϕ as the fraction of surviving species in the following. For the case of symmetric couplings, $\Gamma = 1$, equations (19)–(21) are identical to those found in replica-symmetric studies of the statics of the model [7], for $p = 2$ they further coincide with the ones reported in [5]. They are readily solved numerically (in terms of κ, q and χ) for arbitrary values of the model parameters u and Γ (at fixed p)[1]. Results for the order parameter q are depicted for the model with pairwise interaction ($p = 2$) in figure 1. We find near-perfect agreement between the analytical theory and numerical simulations[2] for u larger than some critical value $u_c(\Gamma)$ (for $\Gamma < \Gamma_c(u)$ respectively in the right panel of figure 1). The deviations from the theory below u_c (respectively above Γ_c) are due to a breakdown of some of our assumptions regarding ergodicity and the stability of the fixed points, the resulting phase transitions will be discussed in more detail below. Let us finally, in this section, turn to an interpretation of the order parameter q, which within the fixed-point ansatz is given by $q = \lim_{N\to\infty} N^{-1} \sum_i \overline{\langle x_i^2 \rangle}$. If the x_i were normalized to 1 instead of N, q would be closely related to what is known as Simpson's index of diversity [22] and would indicate the probability that two randomly selected individuals of the eco-system are of the same species. A Simpson index of zero thus indicates infinite diversity, a value of 1 corresponds to no diversity. A similar interpretation holds for the normalization of the $\{x_i\}$ used here: finite values of q indicate the co-existence of an extensive number of species with concentrations $x_i \sim \mathcal{O}(N^0)$, while a divergence in q signals the dominance of a sub-extensive number of species with diverging concentrations in the thermodynamic limit [8]. $1/q$ is thus a measure for the diversity of the system, and we expect the behaviour of $1/q$ to be similar to that of the fraction of surviving species $\phi \equiv \int Dz\Theta[x(z)]$. This is indeed confirmed in numerical simulations (not shown here) in which one verifies that $1/q$ and ϕ show the same qualitative behaviour as functions of the model parameters. The left panel of figure 1 thus confirms the role of u as a co-operation pressure, the higher the value of u the more species survive in the long-term limit and the more diverse the system is in its stationary state. The influence of the symmetry of the interactions on the diversity (right panel of figure 1) will be discussed below.

3.3. Stability analysis and phase transitions

Our theory and solution crucially rely on the assumptions made with respect to ergodicity, weak long-term memory, and the stability of the fixed point which the dynamics is assumed to approach asymptotically. A breakdown of this theory may thus be signalled by the failure of any of these assumptions, marking a dynamical phase transition at which the ergodic fixed-point regime ceases to exist. In general, one may imagine the following phenomena to occur:

(i) The analytical ergodic theory resulting in equations (18) might predict the integrated response χ to diverge in some subset of the parameter space of the model. Such a transition has been observed in replicator models with Hebbian interactions [28], and below this transition the system is found to be non-ergodic.

[1] Note here that the right-hand sides of (19)–(21) can be written in the closed form as functions of Δ after performing the Gaussian integrals over z. A solution of these equations can thus most efficiently be obtained by expressing $\{u, q, \chi\}$ as functions of Δ, and by subsequently varying Δ [11].

[2] A discretization method similar to that of [6] is used. The typical (effective) time step is of the order of $\Delta t \approx 0.01$–0.1.

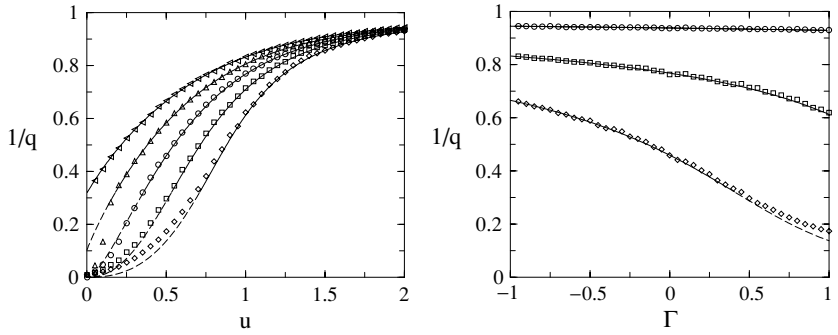

Figure 1. Inverse order parameter q for the model with $p = 2$. Symbols are from simulations for $N = 300$ species, run for 20 000 discretization steps (effective time-stepping is of the order of 0.01–0.1) and averaged over 50 samples of the disorder. Measurements are taken in the last quarter of the simulations. Initial conditions correspond to a flat distribution over the interval $[0, 2]$. The solid lines represent the analytical predictions in the ergodic phase, and have been continued as dashed lines into the region of broken ergodicity, where our theory is no longer valid. Left: $1/q$ as a function of u for $\Gamma = -1, -0.5, 0, 0.5, 1$ from top to bottom. Right: same quantity as a function of Γ at fixed $u = 2, 1, 0.5$ (top to bottom).

(ii) In a similar way the theory might *analytically* predict singularities in either q or κ. No such types of transitions seem to have been observed so far in studies of RRM[3].

(iii) The set of equations (18) might fail to have solutions for certain values of the control parameters, so that no ergodic states are allowed in this region of the phase diagram. We will discuss cases of this type in section 4.

(iv) Our ergodic theory is based on the assumption that all trajectories of the system will evolve into fixed points asymptotically. An onset of instability of these fixed points against small perturbations will thus signal the breakdown of our theory as they will no longer be local attractors of the dynamics. Such transitions have been observed in RRM with Gaussian and Hebbian couplings in [5, 6, 28].

(v) Finally a breakdown of our requirement that long-term memory be weak would indicate that the system remembers perturbations during the transient dynamics. Even if the system still evolves into a fixed point the latter might no longer be unique and the choice of the asymptotic stationary state might thus depend on initial conditions or perturbations at early stages of the temporal evolution. This type of transition has been related to the previous one (instability of the assumed fixed point) in [28], and we will demonstrate below that the conditions for both types of transitions are indeed fulfilled at the same points in parameter space whenever a replicator system with symmetric couplings is considered.

Transitions of the types (i)–(iii) are easily detected in numerical solutions of equations (19)–(21) (or their analogues for other types of RRMs). In the following we will therefore focus on (iv) and (v) and will derive explicit conditions for the onsets of instability and of memory at finite integrated response respectively.

[3] Phases in which $\lim_{N\to\infty} q^{-1} = 0$ have been hinted at in [7] and will be discussed in more detail below. Note however that in these cases the equations describing the ergodic states do not analytically lead to singularities in q, but do not allow for any solutions at all in the phases where q is found to diverge in simulations; they are of the type (iii) in the above list of possible transitions.

3.3.1. Instability of the fixed point To inspect the stability of the assumed fixed point, we will follow [5] and add a small component $\varepsilon\zeta(t)$ of white noise to the system (with $\langle\zeta(t)\rangle = 0$, $\langle\zeta(t)\zeta(t')\rangle = \delta(t-t')$) and then study small fluctuations $\varepsilon y(t)$ and $\varepsilon v(t)$ of the effective species concentration and the single-particle noise about their respective fixed points x and η:

$$x(t) = x + \varepsilon y(t), \qquad \eta(t) = \eta + \varepsilon v(t). \tag{22}$$

In the following we will consider only the case $x > 0$, as it turns out that the onset of instability in replicator systems is determined by the fixed points different from zero while the zero fixed points remain stable against perturbations (see also [5, 28]). Inserting (22) into the effective process (7) (for fixed points $x > 0$) and adding the additional noise component leads to

$$\frac{\mathrm{d}}{\mathrm{d}t}y(t) = -x\left[2uy(t) - \Gamma\frac{p(p-1)}{2}q^{p-2}\int_{-\infty}^{t}\mathrm{d}t'G(t-t')y(t') + v(t) + \zeta(t)\right] \tag{23}$$

to first order. In Fourier space one has

$$\widetilde{y}(\omega) = -\frac{\widetilde{v}(\omega) + \widetilde{\zeta}(\omega)}{\mathrm{i}\omega/x + 2u - \Gamma(p(p-1)/2)\,q^{p-2}\widetilde{G}(\omega)} \tag{24}$$

with $\{\widetilde{y}(\omega), \widetilde{v}(\omega), \widetilde{\zeta}(\omega), \widetilde{G}(\omega)\}$, the Fourier transforms of the one-time functions $\{y(t), v(t), \zeta(t), G(\tau)\}$. Focusing on $\omega = 0$, one obtains

$$\langle|\widetilde{y}(\omega=0)|^2\rangle_\star = \phi \times [\langle|\widetilde{v}(\omega=0)|^2\rangle_\star + 1]\frac{\chi^2}{\phi^2}. \tag{25}$$

The first factor of ϕ in (25) takes into account that (24) was derived for non-zero fixed points $x > 0$ and that fluctuations about zero fixed points do not contribute to $\langle|\widetilde{y}(\omega=0)|^2\rangle_\star$. We have also used equation (21) to replace $(2u - \Gamma p(p-1)q^{p-2}\chi/2)^{-2}$ by χ^2/ϕ^2. The self-consistency condition on the covariance of the single-particle noise (equation (8)) on the other hand implies

$$\langle|\widetilde{v}(\omega)|^2\rangle_\star = \frac{p(p-1)}{2}q^{p-2}\langle|\widetilde{y}(\omega)|^2\rangle_\star \tag{26}$$

Insertion of (26) into (25) then allows one to solve for $\langle|\widetilde{y}(0)|^2\rangle_\star$, and one finds

$$\langle|\widetilde{y}(0)|^2\rangle_\star = \left[\frac{\phi}{\chi^2} - \frac{p(p-1)}{2}q^{p-2}\right]^{-1}. \tag{27}$$

We conclude that $\langle|\widetilde{y}(0)|^2\rangle_\star$ diverges when the square bracket on the right-hand side of (27) vanishes, suggesting an onset of instability. $\langle|\widetilde{y}(0)|^2\rangle_\star$ is predicted to become negative whenever the right-hand side of (27) becomes negative, indicating a further contradiction. The onset of instability thus occurs at the point defined by

$$\frac{p(p-1)q^{p-2}}{2\phi}\chi^2 = 1, \tag{28}$$

and the fixed points are stable whenever this expression is strictly smaller than 1. With some further algebra one can show that (28) defines a line $u_c(\Gamma, p) = u_c(\Gamma = 0, p)(1+\Gamma)$ in the (u, Γ) plane for any fixed value of p.

3.3.2. Memory onset In the previous section we have related the breakdown of our ergodic theory to a local instability of the fixed point reached by the dynamics. We will now inspect for an onset of long-term memory at finite integrated response. This type of transition has been observed previously, for example, in Minority Games with self-impact correction or diluted

interactions [26, 27], and can also be interpreted in terms of a breakdown of time-translation invariance (see [20] for details). It is also found in replicator systems with Hebbian interactions [28]. To see how solutions with memory bifurcate from the time-translation invariant ergodic states, we will proceed along the lines of [20] and make the following ansatz for the response function:

$$G(t,t') = G_0(t-t') + \varepsilon \widehat{G}(t,t'), \tag{29}$$

where $\varepsilon\widehat{G}(t,t')$ is a small contribution which breaks time-translation invariance. The starting point of the dynamics can here no longer be sent to $-\infty$. For a physical interpretation of $\mathbf{G}_0$ and $\widehat{\mathbf{G}}$, see [28]. Following [20] $\widehat{\mathbf{G}}$ is taken to depend only on the (earlier) time t' asymptotically, i.e., $\lim_{t\to\infty}\widehat{G}(t,t') = \widehat{G}(t')$.

Starting from (29), one expands the kernel of the retarded self-interaction in the effective process to linear order in $\widehat{G}$, and finds the following effective process:

$$\frac{\mathrm{d}}{\mathrm{d}t}x(t) = -x(t)\Bigg[2ux(t) - \Gamma\frac{p(p-1)}{2}\int_0^t \mathrm{d}t' G_0(t-t')C(t-t')^{p-2}x(t') \tag{30}$$

$$- \varepsilon\Gamma\frac{p(p-1)}{2}\int_0^t \mathrm{d}t'\widehat{G}(t')C(t-t')^{p-2}x(t') + \eta(t) - \kappa(t)\Bigg] \tag{31}$$

so that non-zero asymptotic fixed points are now found to fulfil

$$2ux - \Gamma\frac{p(p-1)}{2}\chi q^{p-2}x - \varepsilon\Gamma\frac{p(p-1)}{2}\int_0^t \mathrm{d}t'\widehat{G}(t')q^{p-2}x(t') + \left(\frac{p}{2}q^{p-1}\right)^{1/2} z - \kappa = 0. \tag{32}$$

From this one can compute the response function $\widehat{G}(t'')$ at a transient time t'' self-consistently and finds

$$\widehat{G}(t'') = \Gamma\frac{p(p-1)}{2}q^{p-2}\left(2u - \Gamma\frac{p(p-1)}{2}\chi q^{p-2}\right)^{-1}\int_0^t \mathrm{d}t'\widehat{G}(t')\left\langle\frac{\delta x(t')}{\delta h(t'')}\right\rangle_\star. \tag{33}$$

This can be understood as an eigenvalue problem of the form $\widehat{G}(t) = \int \mathrm{d}t' M(t-t')\widehat{G}(t')$, with a suitable kernel $\mathbf{M}$ [20]. Upon taking Fourier transforms and focusing on the zero frequency mode $\omega = 0$, one finds after some simplifications

$$\widehat{\chi} = \Gamma\frac{p(p-1)}{2\phi}q^{p-2}\chi^2\widehat{\chi} \tag{34}$$

with $\widehat{\chi} = \int \mathrm{d}t\widehat{G}(t)$. Although $\widehat{\chi} = 0$ is always a solution, one realizes that non-zero solutions for $\widehat{\chi}$ become possible at the point at which

$$\Gamma\frac{p(p-1)q^{p-2}}{2\phi}\chi^2 = 1. \tag{35}$$

We will refer to this as the memory onset (MO) condition in the following.

4. Phase diagram and discussion of results

We now turn to a discussion of the resulting phase diagrams, as depicted in figure 2. In general, we find that our ergodic fixed-point ansatz is valid and stable for values $u > u_c$ with some u_c critical value which depends on the order of interaction p and on the symmetry parameter Γ. Above u_c the system evolves into a unique fixed point, with virtually all species surviving in the limit $u \to \infty$. This corresponds to a fixed point in the interior of the simplex defined by

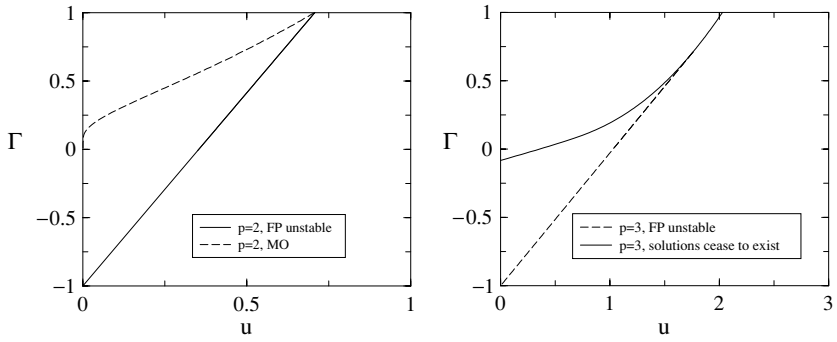

Figure 2. Phase diagrams for the models with $p = 2$ and $p = 3$ in the (u, Γ) plane. Left panel ($p = 2$): the dashed line marks the onset of long-term memory, see equation (35); the solid line marks the onset of the instability of the fixed points, equation (28). Right panel ($p = 3$): the solid curve separates the region in which equations (19)–(21) admit a solution (high u) from the region in which no solutions are found, the dashed line marks the onset of instability, equation (28).

the condition $N^{-1}\sum_i x_i = 1$. For small values of u fewer species survive so that the system operates near the boundary of this simplex.

The dependence of the phase diagram on Γ is particularly interesting. One notes that both conditions (28) and (35) coincide for symmetric couplings $\Gamma = 1$, but that the onset of the instability of the fixed point occurs before memory sets in for $\Gamma < 1$.[4] At the same time, simulations reveal different types of behaviour below the transition, depending on the symmetry of the interactions: while for fully symmetric interactions $\Gamma = 1$ the system reaches a fixed point also below u_c , fixed points are not necessarily observed below u_c for even partially asymmetric couplings. This will be discussed in more detail below. The type of transition also depends on whether the interactions are pairwise or cubic; we find that in the system with $p = 2$ the number of surviving species is always extensive for any $u > 0$, whereas this number can turn out to be $\mathcal{O}(1)$ in the model with $p = 3$ below the transition even in the thermodynamic limit. In the following we will treat the cases $p = 2$ and $p = 3$ separately.

4.1. Pairwise interaction ($p = 2$)

We find here that equations (19)–(21) admit solutions for all u and Γ and we observe no singularities in any of the persistent order parameters. The predictions of the analytical theory for the order parameters in the ergodic phase are compared with numerical simulations in figure 1 and we find near-perfect agreement in the ergodic phases ($u > u_c(\Gamma)$ and $\Gamma < \Gamma_c(u)$, respectively).

The only possible violations of our assumptions of the ergodic stationary state are instabilities of the fixed points or an onset of long-term memory at finite susceptibility χ. The condition for onset of the instability of the fixed points (28) reduces to $u_c(p = 2, \Gamma) = (1 + \Gamma)/(2\sqrt{2})$, as already derived in [5]. If one ignores this instability and continues the solutions of (19)–(21) to the right of the line $u = u_c(p = 2, \Gamma)$, one finds that the memory onset condition (35) is fulfilled along the dashed line in the left panel of figure 2. As the fixed points are already unstable in this regime, this line has no direct physical meaning though,

[4] The equivalence of the MO and instability conditions at $\Gamma = 1$ can be extended to more general replicator equations derived from a Lyapunov function.

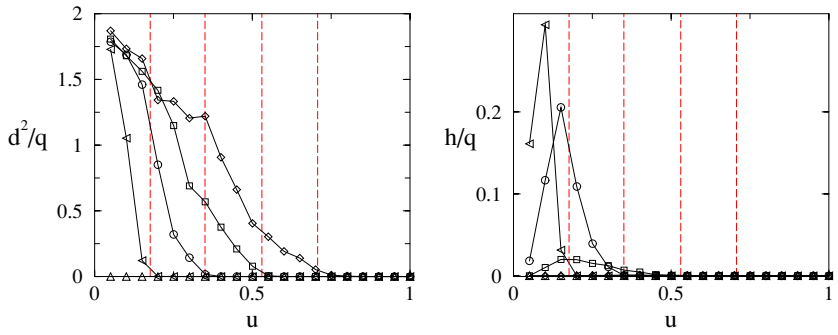

Figure 3. Relative distance d^2/q and roughness h/q versus u for the model with $p = 2$. Connected symbols are from simulations (triangle up: $\Gamma = -1$; triangle left: $\Gamma = -0.5$; circles: $\Gamma = 0$; squares: $\Gamma = 0.5$; diamonds: $\Gamma = 1$). The distance d^2 is obtained by comparing the stationary states of two runs at fixed disorder started from independent random initial conditions over $[0, 2]$. Simulation parameters are shown in figure 1. Vertical dashed lines indicate the location of the phase transitions as predicted by the theory for $\Gamma = -0.5, 0, 0.5, 1$ from left to right. No transition occurs for $u > 0$ and $\Gamma = -1$.

and is depicted only for illustration. We note that for $\Gamma = 1$ both the instability of the fixed point and the onset of memory occur at the same value of $u = 1/\sqrt{2}$. In the statics a de Almeida–Thouless instability is found at this point and replica symmetry is broken at smaller values of u [13]. Interestingly, one does not find any transition at any positive co-operation pressure $u > 0$ for full anti-correlation $\Gamma = -1$, i.e. in the case of zero-sum games.

To verify the onset of non-ergodicity further, we have performed simulations in which two copies of the system with the same realization of the disorder are generated and in which the dynamics is started from two independent sets of random initial conditions drawn from a flat distribution over $x_i(0) \in [0, 2]$. The two resulting trajectories of the system are labelled by $\{x_i^a(t)\}$ and $\{x_i^b(t)\}$, respectively, and we have measured the squared distance $d^2 = N^{-1} \sum_i \left(x_i^a(t) - x_i^b(t)\right)^2$ in the stationary state. Results are depicted in figure 3 (left panel). For convenience we plot the re-scaled distance d^2/q. We find that d^2 is essentially zero above $u_c(\Gamma)$, confirming the ergodicity and independence of the stationary state on initial conditions in this regime. Below u_c we find that $d^2 > 0$, indicating the existence of multiple stationary states and the pronounced relevance of initial conditions. For $\Gamma = -1$ no memory effects are observed at any $u > 0$ as expected from the theory.

We have secondly measured the relative 'roughness' h/q of the trajectories, where $h = N^{-1} \sum_i (\langle x_i(t)^2 \rangle_t - \langle x_i(t) \rangle_t^2)$ and $\langle \cdots \rangle_t$ denotes a time average in the stationary state. As shown in the right panel of figure 3 all trajectories are flat ($h = 0$) irrespective of Γ above $u_c(\Gamma)$, verifying that the system indeed evolves into a fixed point in this regime. For symmetric couplings $\Gamma = 1$ fixed points are also reached below the transition. For $-1 < \Gamma < 1$ we find non-zero values of h below the transition so that we conclude that the system does not necessarily evolve into fixed points here[5]. This behaviour is also confirmed in figure 4, where we show typical trajectories of the system at $\Gamma = 0$ (fully uncorrelated couplings) below and

[5] The numerical data for h appears to show some dependence on system size, running time and time-window over which measurements are taken in the regime of volatile trajectories below $u_c(\Gamma < 1)$ (i.e., when $h > 0$). The observations that fixed points are attained for all Γ above u_c and for all u for $\Gamma = 1$ are, however, not affected. More extensive simulations seem appropriate in order to check whether the apparently decreasing values of h as u approaches zero at $\Gamma < 1$ are genuine or a numerical artifact.

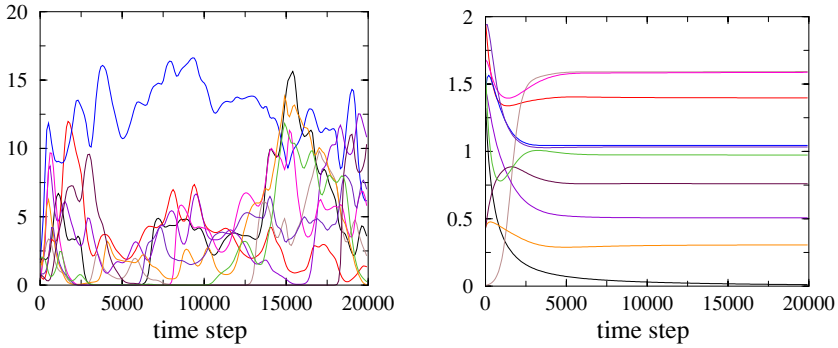

Figure 4. Trajectories $\{x_i(t)\}_t$ for 10 individual species in single runs of simulations of the model with $p = 2$ at fully asymmetric couplings, $\Gamma = 0$. Left: $u = 0.2$ below the transition, where fixed points are unstable; right: $u = 1.0$ above the transition. Simulations are for $N = 500$ agents runs for 20 000 time steps.

above and the transition, see also [6] for a similar figure. For $\Gamma = 1$ one finds that the system evolves into a fixed point irrespective of u (trajectories not shown here).

We conclude the section concerning the model with $p = 2$ by a brief summary of the effects of asymmetry in the couplings. As discussed above even partial asymmetry changes the nature of the phase transition as compared to the fully symmetric case. This was already pointed out in [5, 6]. For symmetric couplings the system evolves into a fixed point asymptotically both above and below $u_c(\Gamma = 1) = 1/\sqrt{2}$. Below the transition fixed points are however not unique, hence the breaking of ergodicity and dependence on initial conditions. For $\Gamma < 1$ we find that the system reaches a fixed point asymptotically above $u_c(\Gamma)$, but not necessarily below, where instead one finds volatile trajectories in which species can almost die out and then recover to large concentrations at later times. No transition is observed for $\Gamma = -1$ (full anti-correlation), and the system here evolves into a unique fixed point for all $u > 0$. The effects of asymmetry on the diversity $1/q$ are demonstrated in figure 1 (right panel). Generally speaking, asymmetry increases the diversity of species in the stationary state (equivalently decreasing Γ leads to a higher fraction of surviving species). While this effect is small for large values of u some significant dependence on Γ is observed for small co-operation pressure u.

Finally, the effects of asymmetry on the fitness of the species in the stationary state are demonstrated in figure 5. The average fitness is here given by $f = N^{-1}\sum_i x_i f_i[\mathbf{x}]$ with $f_i[\mathbf{x}] = -2ux_i - \sum_j J_{ij}x_j$, and it turns out that $f_i \equiv f$ for all surviving species i. From the analytical calculation one finds $f = -\kappa$. As shown in the figure an increased asymmetry in the couplings leads to a reduced overall fitness. Again the effect is strong for small u but negligible for large co-operation pressure (where the diagonal term proportional to u dominates the interactions). Thus, in systems with symmetric couplings fewer species tend to survive than in systems with uncorrelated or anti-correlated interactions, but these surviving species have higher fitness than the many survivors of systems with asymmetric or anti-symmetric couplings.

4.2. Cubic interaction ($p = 3$)

For $p = 3$ we find a distinctively different behaviour of the system. Equations (19)–(21) admit solutions only for $u > u^*(\Gamma)$, and below this value no ergodic fixed-point solutions can

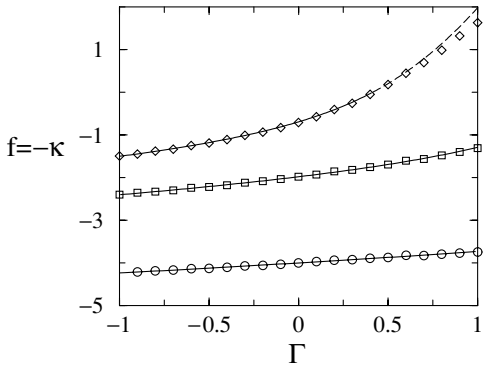

Figure 5. Average fitness $f = -\kappa$ versus Γ for the model with $p = 2$. Symbols are from simulations ($u = 0.5, 1, 2$ from top to bottom), simulation parameters as in figure 1. The solid line marks the predictions of the analytical theory, for $u = 0.5$ the theoretical line has been continued as dashed line into the phase where the ergodic theory is no longer valid.

be found. The obtained value $u^*(\Gamma = 1) \approx 2.028$ has already been reported in the context of a replica analysis of the model with symmetric couplings [7]. Note also that the limits $\lim_{u\downarrow u^*} q$, $\lim_{u\downarrow u^*} \chi$ and $\lim_{u\downarrow u^*} \kappa$ exist and take finite values. As indicated in figure 2 this type of transition is preceded by an onset of instability of the fixed points (determined by equation (28)) for values of $\Gamma < \Gamma_0 \approx 0.7$ in the sense that the instability sets in as u is lowered starting in the ergodic phase before solutions of the saddle point equations cease to exist. We note that the onset of instability again occurs along a line in the (u, Γ) plane, with $u_c(p = 3, \Gamma) = u_c(p = 3, \Gamma = 0)(1 + \Gamma)$, where $u_c(p = 3, \Gamma = 0) \approx 1.028$.[6] We find that solutions of the saddle-point equations exist for all $u > 0$ if Γ is (sufficiently) negative [7].

Results from numerical simulations of the model with $p = 3$ are presented in figure 6. Given the cubic interaction, we limit ourselves to relatively small system sizes $N = 200$ and to moderate running times here. Results in the ergodic phases are, however, not affected significantly by these constraints in computing time. We observe good agreement between the results for the order parameter q as obtained from theory and experiment in the ergodic region, with only slight discrepancies close to the transitions due to finite-size effects. Again asymmetry in the couplings increases the diversity and number of surviving species. The right panel of figure 6 confirms that non-ergodicity sets in at $u_c(\Gamma)$, indicated by non-zero distances between the stationary states obtained when starting the dynamics at fixed disorder from different random initial conditions as explained above.

To summarize we have found a regime $u > \max(u_c(\Gamma), u^*(\Gamma))$ in which our ergodic theory applies and matches the simulations. For $\Gamma < \Gamma_0$ we then find an intermediate regime $u_* < u < u_c$ in which solutions of the saddle point equations exist, but in which the attained

[6] It turns out that equations (19)–(21) have two branches of solutions above u^*, both solutions merge at u^*. For $\Gamma > \Gamma_0$ we find that the fixed points are stable along the physical branch and that condition (28) for the onset of instability is fulfilled at $u_c(p = 3, \Gamma) = u_c(p = 3, \Gamma = 0)(1 + \Gamma)$ only along the unphysical branch. Thus, no instability is observed and a transition of the above type (iii) is the first one to occur when u is lowered from infinity. For $\Gamma < \Gamma_0$ the fixed point becomes unstable along the physical branch and the instability transitions precedes the failure of solutions to exist.

[7] Some numerical inaccuracies are encountered for $\Gamma \approx 0$ when determining the line along which solutions cease to exist. The solid line in the phase diagram for $p = 3$ (right panel of figure 2) could therefore be investigated more carefully near $\Gamma = 0$. At this point instabilities of the fixed points have already set in and solutions are unphysical, so that the precise location of the point at which solutions cease to exist is immaterial for the behaviour of the model.

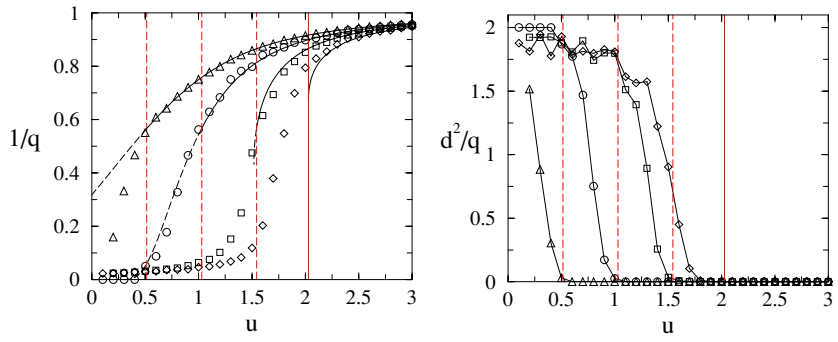

Figure 6. Reciprocal order parameter q and distance d^2/q versus u for the model with $p = 3$. Symbols are from simulations (triangles: $\Gamma = -0.5$; circles: $\Gamma = 0$; squares: $\Gamma = 0.5$; diamonds: $\Gamma = 1$). Solid lines for $1/q$ are the analytical predictions in the ergodic phase $u > u_c$, continued as dashed lines into the non-ergodic phases. Vertical lines indicate the predicted locations of the transitions. Simulations were performed for $N = 200$ species, started from random initial conditions drawn with flat distribution from $x_i(0) \in [0, 2]$ and run for 3000 time steps. Results are averages over 20 samples of the disorder.

fixed points are unstable and the stationary state depends on initial conditions. No such intermediate regime appears to be found for $\Gamma > \Gamma_0$. Finally, below u^* no solutions of the equations for the order parameters in the stationary ergodic state exist. The transition at u^* is not marked by any divergence in the analytic solutions for (q, χ, κ) as $u \downarrow u^*$. To conclude this section, we report some indications about the behaviour of the system below u^* based on numerical simulations (we restrict to $\Gamma = 1$). While the persistent order parameters converge to finite values in the limit of large N above u^*, we observe strong finite size effects for $u < u^*$. The numerical data are consistent with power law behaviour $q \sim N^{\gamma}$ and $\phi \sim N^{\delta}$ with $\gamma > 0$ and $\delta < 0$ below u^* (see figure 7). This divergence of q with N seems to suggest that only a sub-extensive number of species $\phi N \sim N^{1+\delta}$ survives in this regime ($\delta < 0$) in the thermodynamic limit. Given the constraint $\lim_{N\to\infty} N^{-1} \sum_i x_i = 1$, we then conclude that these surviving species each must have concentrations scaling as $x_i \sim N^{-\delta}$, which in turn results in $q = N^{-1} \sum_i x_i^2 \sim N^{-\delta}$, i.e. we expect $\gamma = -\delta$. Within the accuracy of our simulations this is indeed what we observe (see figure 7). More precisely our simulations are consistent with $\gamma = -\delta = 1$ at low values of u, so that we expect only a *finite* number of species to survive in this regime ($\phi N \sim \mathcal{O}(N^0)$), even in the thermodynamic limit. This unusual effect is indeed confirmed upon plotting the number of species which are still alive as a function of time for different system sizes (see the right panel of figure 7). Closer inspection shows that the final number of surviving species in these simulations all fall into the range $10 \leqslant N\phi \leqslant 12$ even if the system size is varied by a factor of 4 from $N = 50$ to $N = 200$. A similar effect was observed in a replicator model with an explicit extinction threshold [14].

While our simulations confirm convincingly that $\gamma = -\delta = 0$ above u^*, and while they seem to suggest that $\gamma = -\delta = 1$ sufficiently far below the transition, the accuracy of our numerical experiments do not allow us to make any statement as to whether this onset of non-extensivity occurs continuously or discontinuously, i.e., whether the exponents drop instantly to zero when the transition at $u = u^*$ is crossed (from below) or whether one observes a crossover.

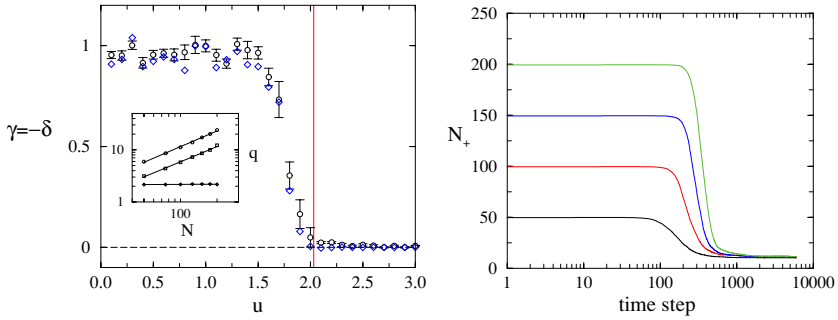

Figure 7. Left: Exponents γ (circles) and $-\delta$ (diamonds) (see text) as functions of u for the model with $p = 3$ ($\Gamma = 1$). Each data point is obtained by performing simulations at fixed u for $N = 50, 75, \ldots, 200$, simulations are run for 6000 steps, averages over 10 samples of the disorder are taken, and subsequent fits to power laws $q \sim N^{\gamma}$ and $\phi \sim N^{\delta}$ are performed to obtain γ and δ. Vertical bars indicate the standard error of γ. Vertical solid line marks $u^*(\Gamma = 1)$. Inset: Log–log plots of q versus N for $u = 1.0$ (circles), $u = 1.5$ (squares) and $u = 2.5$ (diamonds) and the corresponding fits to power laws. (The data for q at $u = 2.5$ in the inset have been multiplied by a factor of 2 for convenience.) Right: temporal evolution of the number N_+ of species with concentration $x_i(t) > 0.01$ for the same parameters, and at $u = 1$. Different curves are obtained from simulations of different system sizes $N = 50, 100, 150, 200$ from bottom to top.

5. Concluding remarks

In summary, we have demonstrated how generating functionals can be used to study random replicator models. In the case of symmetric couplings this approach is able to reproduce the equations describing the ergodic stationary states obtained from static replica studies, but in addition the analysis of the dynamics also allows to address replicator systems with asymmetric interactions and to make accurate analytical predictions for the order parameters in their fixed-point regimes and the resulting phase diagrams.

Our analysis of Gaussian RRM indicates that the effect of asymmetry and anti-symmetry in the couplings is to increase the stationary value of the diversity parameter $1/q$ and with it the number of surviving species. This is the case for both models studied here, with interactions between $p = 2$ and $p = 3$ species, respectively. Asymmetry in the couplings also reduces the fitness of the surviving species. Furthermore, the range of the ergodic phase seems to be consistently larger, the higher the degree of anti-symmetry in the couplings becomes. The symmetry or otherwise of the interactions also determines the behaviour of the system in the non-ergodic phases. Replicators with symmetric couplings evolve into fixed points in all regions of the phase diagram. In the symmetric case one expects a large number of such fixed points in the phase below u_c [4], and initial conditions determine which of these is reached, as indicated by the memory-onset. No such phase (and hence no MO transition) is found in models with asymmetric or anti-symmetric couplings. Instead, volatile trajectories are here observed below the transition, and individual species may come close to extinction $x_i(t) \ll 1$, but then recover to macroscopic values $x_i(t) \sim \mathcal{O}(1)$.

Models in which the self-interaction is of a lower order than the terms coupling distinct species appear to exhibit a phase in which the fraction of surviving species scales as $\phi \sim 1/N$ so that only a *finite* number of species survives in the long run even in the thermodynamic limit. Possibly parallels with condensation effects in growth models of complex networks with quenched fitnesses of links and/or nodes can be drawn, as the dynamics of such networks obeys growth laws which are similar to the replicator equations studied here [29, 30].

While we have here concentrated on relatively simple single-population systems with Gaussian couplings, similar approaches may be taken to address more intricate models of replicators. These could include multi-population models of game theory or dynamical models of chemical metabolic reactions, which progress in proportion to the concentration of reaction partners and in which stoichiometric coefficients might be modelled in terms of quenched random couplings. Multi-population replicator equations of game theory correspond to so-called bi-matrix games [3], and it would here be interesting to study the relation between the fixed points of the replicator dynamics and the Nash equilibria of such games [31], also as a function of the degree of anti-correlation in the payoff matrices and the co-operation pressure. Some work is currently in progress along these lines.

Acknowledgmets

This work was supported by the European Community's Human Potential Programme under contract HPRN-CT-2002-00319, STIPCO. The author thanks G Bianconi, A C C Coolen, M Marsili and D Sherrington for helpful discussions.

References

[1] Hofbauer J and Sigmund K 1988 *Dynamical Systems and the Theory of Evolution* (Cambridge, UK: Cambridge University Press)
[2] Peschel M and Mende W 1986 *The Prey–Predator Model* (Berlin: Springer)
[3] Weibull J W 2002 *Evolutionary Game Theory* (Cambridge, MA: MIT Press)
[4] Diederich S and Opper M 1989 *Phys. Rev.* A **39** 4333
[5] Opper M and Diederich S 1992 *Phys. Rev. Lett.* **69** 1616
[6] Opper M and Diederich S 1999 *Comput. Phys. Commun.* **121–122** 141
[7] de Oliveira V and Fontanari J 2000 *Phys. Rev. Lett.* **85** 4984
[8] de Oliveira V and Fontanari J 2001 *Phys. Rev.* E **64** 051911
[9] de Oliveira V and Fontanari J 2002 *Phys. Rev. Lett.* **89** 148101
[10] de Oliveira V 2003 *Eur. Phys. J.* B **31** 259
[11] Santos D and Fontanari J 2004 *Phys. Rev.* E **70** 061914
[12] Tokita K 2004 *Phys. Rev. Lett.* **93** 178102
[13] Biscari P and Parisi G 1995 *J. Phys. A: Math. Gen.* **28** 4697
[14] Tokita K and Yasumoti A 1999 *Phys. Rev.* E **60** 842
[15] Chawanya T and Tokita K 2002 *J. Phys. Soc. Japan* **71** 429
[16] Rieger H 1989 *J. Phys. A: Math. Gen.* **22** 3447
[17] De Dominicis C 1978 *Phys. Rev.* B **18** 4913
[18] Mezard M, Parisi G and Virasoro M 1987 *Spin Glass Theory and Beyond* (Singapore: World Scientific)
[19] Challet D, Marsili M and Zhang Y-C 2005 *Minority Games* (Oxford: Oxford University Press)
[20] Coolen A C C 2005 *The Mathematical Theory of Minority Games* (Oxford: Oxford University Press)
[21] Johnson N F, Jefferies P and Hui P M 2003 *Financial market complexity* (Oxford: Oxford University Press)
[22] Simpson E H 1949 *Nature* **163** 688
[23] Heerema M and Ritort F 1999 *Phys. Rev.* E **60** 3646
[24] Crisanti A, Horner H and Sommers H-J 1193 *Z. Phys.* B **92** 257
[25] Eissfeller H and Opper M 1992 *Phys. Rev. Lett.* **68** 2094
[26] Heimel J A F and De Martino A 2001 *J. Phys. A: Math. Gen.* **34** L539
[27] Galla T 2005 *J. Stat. Mech.* P01002
[28] Galla T 2005 *J. Stat. Mech.* P11005
[29] Bianconi G and Barabasi A-L 2001 *Phys. Rev. Lett.* **86** 5632
[30] Bianconi G 2004 *Preprint* cond-mat/0412399
[31] Berg J M and Weigt M 1999 *Europhys. Lett.* **48** 129